Concise Chemoenzymatic Total Synthesis and Identification of Cellular Targets of Cepafungin I

Alexander Amatuni, Anton Shuster, Alexander Adibekian*, Hans Renata*

[*] Alexander Amatuni, Anton Shuster, Prof. Dr. Alexander Adibekian, Prof. Dr. Hans Renata
Department of Chemistry, The Scripps Research Institute
130 Scripps Way, Jupiter, FL 33458 (USA)
E-mail: aadibeki@scripps.edu, hrenata@scripps.edu

Supporting information for this article is given via a link at the end of the document

Abstract: The natural product cepafungin I was recently reported to be one of the most potent covalent inhibitors of the 20S proteasome core particle through a series of in vitro activity assays. Here, we report a short chemoenzymatic total synthesis of cepafungin I featuring the use of a regioselective enzymatic oxidation to prepare a key hydroxylated amino acid building block in a scalable fashion. The strategy developed herein enabled access to a chemoproteomic probe, which in turn revealed the exceptional selectivity and potency of cepafungin I towards the β2 and β5 subunits of the proteasome. Further structure-activity relationship studies suggest the key role of the hydroxyl group in the macrocycle and the identity of the lipid tail in modulating the potency of this natural product family. This study lays the groundwork for further medicinal chemistry exploration to fully realize the anticancer potential of cepafungin I.

Introduction

Cepafungin I and glidobactin A are two macrolactams belonging to a larger family of natural products called the syrbactins (**Fig. 1**). Members of this family share a common 12-membered macrolactam core consisting of a vinylogous amino acid and a lysine residue that may exist in various oxidation states. Further diversity can be found within the tail portion of the natural products: while the cepafungins and the glidobactins possess unsaturated fatty acid tails, all syrbactins contain a Val-Val unit that is linked via a unique ureido moiety.[1] Initial biological evaluation suggested that the glidobactins and the cepafungins exhibit moderate antifungal activity and potent antitumor activity against P388 leukemia in mice.[2a,b] More recently, it has been determined that the latter activity arises from inhibition of the 20S proteasome core particle (CP) via covalent engagement of two distinct catalytically-active Thr1O$^{\gamma}$ residues by the unsaturated lactam motif of the macrocycle.[3] Cepafungin I, in particular, exhibits remarkably strong inhibitory activity relative to all known proteasome inhibitors to date (IC_{50} of 4 nM against the β5 subunit of yeast CP).[4] The proteasome is a multiprotein complex that plays a critical role in protein degradation. Given the centrality of the proteasome in the regulation of cell cycle and apoptosis, its inhibition constitutes a promising modality for cancer therapy. In support of this notion, three proteasome inhibitors, bortezomib, carfilzomib and ixazomib, have been approved by the U.S. Food and Drug Administration for the treatment of multiple myeloma. However, both bortezomib and carfilzomib have been reported to exhibit several side effects such as thrombocytopenia and high occurrence of relapse and chemoresistance have also been reported.[5] Thus, there is still an urgent need to advance new proteasome inhibitors as drug candidates that will address these issues.

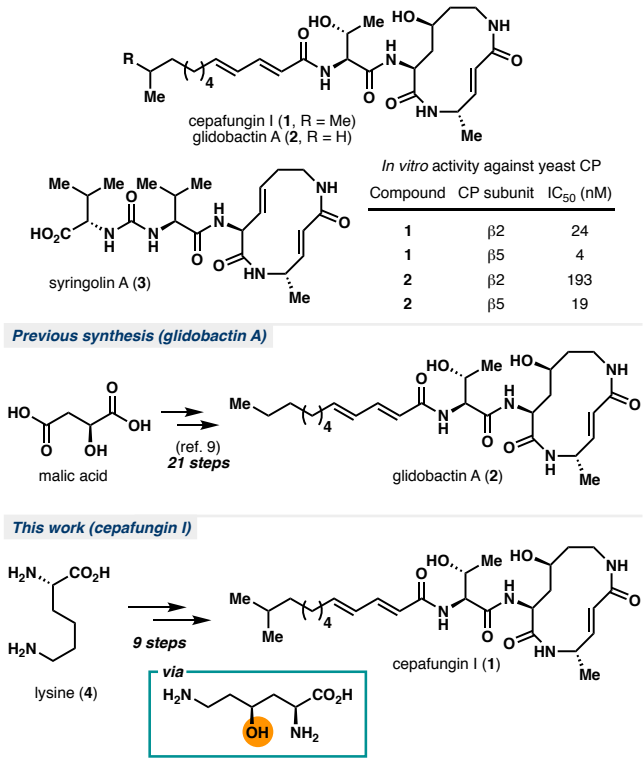

Figure 1. The syrbactins family of natural products, their respective inhibitory activities on the 20S proteasome, prior approach to glidobactin A and our synthetic strategy towards cepafungin I.

Similar to bortezomib, the syrbactins trigger apoptosis by eliciting p53 accumulation and inhibiting NF-κB activity.[1] Pioneering studies by Bachmann and co-workers using a syrbactin derivative additionally showed that while this compound exhibited cytotoxic effects on cancer cell lines, the effect was most pronounced in multiple myeloma.[6] Recent research has begun to elucidate certain resistance mechanisms in multiple myeloma. While current proteasome inhibitors primarily inhibit the β5 subunit, it has been shown that co-inhibition of the β2 subunit prevents recovery of proteasome activity by causing aggregation/inactivation of the proteasomal transcription factor Nrf1. Notably, the cytotoxicities of bortezomib and carfilzomib towards solid tumor cells (e.g., triple negative breast cancer) are significantly enhanced in this manner, whereas either drug had otherwise not shown clinical efficacy on its own. Moreover, co-inhibition of β5 with β2 provides a stronger antineoplastic effect than with β1, highlighting the importance of advancing new proteasome inhibitors with equipotent activity for these subunits.[7,8] Cepafungin I, with its low nanomolar activity towards β5 and β2 (IC50 = 4 nM and 24 nM, respectively), stands as an attractive candidate for such purpose.

A seminal work by Schmidt and coworkers in 1992 established the first total synthesis of glidobactin A.[9] Starting from malic acid, the synthesis of the natural product was achieved in 21 steps. While a landmark achievement, this approach suffers from high step count due to inefficient functional group interconversions and extraneous protecting group manipulations. For example, the synthesis of the key 4-hydroxylysine moiety took place in 12 steps from malic acid, featuring HWE homologation, asymmetric hydrogenation and displacement of the terminal alcohol with NaN_3. Efforts by Ichikawa,[10a,b,c] Pirrung,[11] Stephenson[12] and others[13a,b,c,d] have established viable synthetic routes to the syrbactins. However, these routes would not be amenable to the introduction of the key 2º alcohol within the embedded lysine unit.

Results and Discussion

Similar to previous studies, we recognized that an efficient route to 4-hydroxylysine (or its synthetic equivalent) would hold the key to the development of a practical synthesis of cepafungin I. If such a route could be identified, iterative condensations with alanine and an acetate equivalent would rapidly generate the macrocyclic core of the natural product. We have previously established the biosynthetic origin of the 4-hydroxylysine moiety of glidobactin A.[14] Within the pathway, a nonheme dioxygenase, GlbB, catalyzes the direct C-H hydroxylation of free-standing lysine at the C4 position prior to loading of the product onto the nonribosomal peptide synthetase assembly line. Substrate scope examination of GlbB revealed that while the enzyme exhibits a narrow substrate specificity, it is able to hydroxylate lysine with remarkably high catalytic efficiency. In our hands, however, large-scale biocatalytic hydroxylation with purified GlbB was hampered by poor scalability as the reaction gave poor conversion when conducted at > 100 mg scale. While this issue could be solved by conducting the reaction with clarified lysate of cells expressing GlbB, the poor soluble expression of GlbB led to sub-optimal titer (**Fig. 2**). Gratifyingly, co-expression of chaperones GroES/EL was found to increase soluble expression of GlbB, which translates to ca. 5-fold improvement in reaction conversion and yield on small scale. For large scale reactions, *ca*. 6–7 g of lysine could be fully converted to its C4-hydroxylated counterpart in a single pass with 1 L of clarified cell lysate (final OD_{600} = 12.5), corresponding to a titer of *ca*. 6–7 g/L based on the original volume of the expression culture.

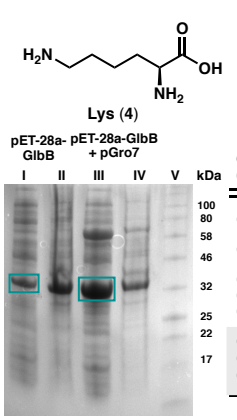

conditions (in lysate)	OD_{600}	[Lys] (mM)	LCMS conversion (%)
GlbB	30	40	71
GlbB	5	40	14
GlbB + GroES/ GroEL	5	40	75
GlbB + GroES/ GroEL[#]	12.5	40	>95

Figure 2. Optimization of preparative scale hydroxylation of **4** with GlbB. Co-expression of chaperones GroES/GroEL was found to improve the soluble expression of GlbB, resulting in ca. 5-fold improvement in reaction conversion. Lanes (I) and (III): soluble fraction, lanes (II) and (IV): insoluble fraction, lane (V): protein ladder. [#]Reaction conducted at 6 gram scale.

Having solved the material throughput issue for the production of **5**, we turned our attention to its conversion to the macrocyclic core of **1**. We have previously described the conversion of **5** to intermediate **6** by way of coupling with alaninol.[14] However, attempts to selectively oxidize the 1º alcohol of **6** were beset by low yields and poor selectivity (**Scheme 1A**). Similarly, attempts to effect differential protections of the α- and ε-amine proved problematic due to the presence of the C4-OH. An alternative route was thus devised to circumvent these issues (**Scheme 1B**). Lactone **7**, prepared routinely on multi-gram scale in 3 steps from lysine, was reacted with Weinreb amide **8** in the presence of $AlMe_3$ to afford dipeptide **9** in 90% yield. Treatment of **9** with $LiAlH_4$ effected a clean reduction of the Weinreb amide moiety to the corresponding aldehyde without any observable over-reduction or side reactivity with any of the carbonyl groups in the molecule. Olefination with Wittig reagent **10** furnished enoate **11**, which constitutes the protected linear form of the target macrocyclic core. As a testament to the robustness of the route, more than 1.5 g of **11** could be prepared in a single pass.

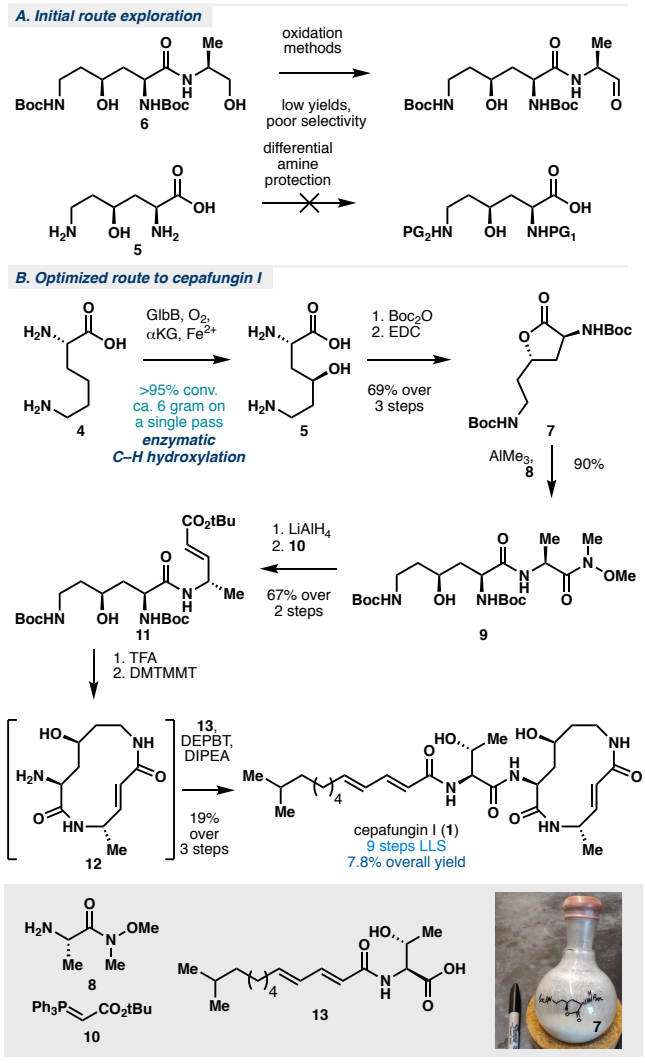

Scheme 1. Chemoenzymatic total synthesis of cepafungin I (**1**) starting from **4**. (A). Failed routes towards **1** from **5** or **6**. (B) Final synthetic route to **1** featuring $AlMe_3$-assisted aminolysis of lactone **7**.

While global deprotection of **11** could be achieved cleanly under acidic conditions, the subsequent macrolactamization step required extensive optimization (See **Table S1** for optimization). This observation was in line with previous efforts in the total synthesis of glidobactin A and the syrbactins where late-stage macrolactamization typically proceeded in less than 30% yield.[9,12,13a,c,d] Eventually, DMTMMT was identified as the optimal coupling reagent, providing ~60% NMR yield of the desired macrolactam.[15] Due to the high polarity of **12**, we elected to bypass any purification step and used the compound in a crude form for subsequent coupling with the fully elaborated tail fragment **13**. Extensive screening of peptide coupling conditions (**Table S2**) eventually identified DEPBT as an optimal coupling reagent for this step, leading to the formation of the target natural product in 19% yield from **11**. Overall, our chemoenzymatic synthesis of cepafungin I proceeded in 9 steps (longest linear sequence) and 7.9% overall yield from lysine. By virtue of this chemoenzymatic strategy, our route provides exceptionally rapid access to the key hydroxylysine residue and overcomes longstanding challenges associated with synthetic access to syrbactins bearing 2º alcohol at the L-lysine fragment. This route also highlights DMTMMT as a superior macrolactamization reagent to construct the strained 12-membered ring. Finally, the modularity of this route enables the rapid construction of synthetic analogs and chemoproteomic probes for further biological evaluation (*vide infra*).

Multiple myeloma (MM) has remained the main indication for clinical trials of novel proteasome inhibitor drug candidates since the FDA approval of the first-in-class drug Velcade (bortezomib) in 2003.[16] Accordingly, we started our biological investigations with cytotoxicity measurements of **1** in the commonly used MM cell lines RPMI 8226 and MM1.R to evaluate its potential as a cancer drug candidate. Cells were treated with various concentrations of **1** for 24 h or 48 h and the percentage of viable cells was determined via the WST-1 assay (**Fig. 3A**). Indeed, **1** proved potently toxic and the measured cytotoxicity after 48 h treatment (EC_{50s} of 31 nM for RPMI 8226 and 23 nM for MM1.R) aligned well with the previously reported data for clinical proteasome inhibitor drugs bortezomib (30 nM for RPMI 8226; 3 nM for MM1.R[17]) and carfilzomib (5 nM for RPMI 8226[18]). Although **1** and structurally related natural products have previously been shown to inhibit proteasomal subunits PSMB2 (β2) and PSMB5 (β5) in purified yeast[4] and mammalian[19] proteasomes, direct target engagement of proteasomes by the syrbactins in mammalian cells has not yet been shown. Accordingly, we decided to perform a deep profiling of cellular targets of **1** using a classical chemoproteomics approach. For this purpose, we synthesized probe **14**, an alkyne-tagged derivative of **1** (**Fig. 3**). RPMI 8226 lysates were treated with increasing concentrations of **14** for 1 h at r.t. and the probe-labeled proteins were then conjugated to TAMRA azide using copper(I)-catalyzed alkyne-azide cycloaddition (CuAAC)[20], separated by SDS-PAGE and visualized by in-gel fluorescence scanning (**Fig. S1A**). The gel profile revealed only a few bands, thus suggesting low proteomic promiscuity of **14**. To examine whether **14** can be used as a clickable analog of **1**, we performed a gel-based competitive profiling experiment. RPMI 8226 cells were treated *in situ* with various concentrations of **1** for 6 h, lysed, and then treated with 10 μM **14** for 1 h, followed by TAMRA conjugation and protein visualization, as described above (**Figs. 3B, S1B**). Excitingly, only a few bands were successfully competed at nanomolar concentrations, suggesting high potency and selectivity of **1** towards its targets. To identify the competed protein targets, we performed an *in situ* competitive LC-MS/MS-based experiment. Briefly, RPMI 8226 cells were treated with 100 nM **1** for 6 hours, lysed, then treated with 10 μM **14** followed by CuAAC-mediated conjugation of biotin azide, enrichment with streptavidin beads, trypsin digestion, and LC-MS/MS analysis. Out of 764 proteins enriched by **14**, only 5 were >50% competed by **1** (**Figs. 3C**, **3D**; **Table S1**). Strikingly, all 5 identified targets were 20S proteasome subunits: PSMB5, PSMB10, PSMA5, PSMB1, and PSMB2. Such high selectivity is remarkable, especially considering that the structure of **1** contains two electrophilic α, β-unsaturated amides that could potentially engage hundreds of reactive cysteines.[21]

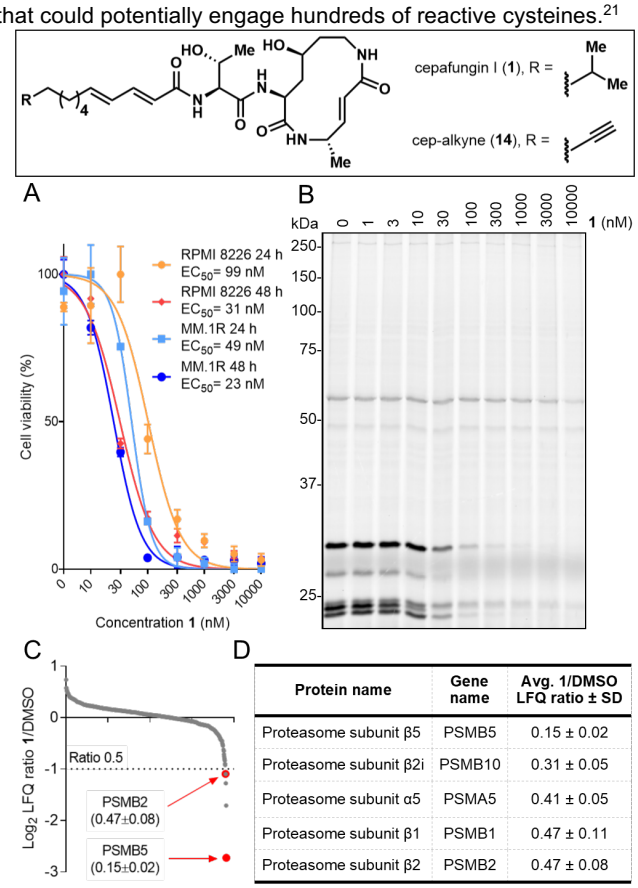

Protein name	Gene name	Avg. 1/DMSO LFQ ratio ± SD
Proteasome subunit β5	PSMB5	0.15 ± 0.02
Proteasome subunit β2i	PSMB10	0.31 ± 0.05
Proteasome subunit α5	PSMA5	0.41 ± 0.05
Proteasome subunit β1	PSMB1	0.47 ± 0.11
Proteasome subunit β2	PSMB2	0.47 ± 0.08

Figure 3. Cytotoxicity and cellular target identification of cepafungin I. (A) Cytotoxicity curves of RPMI 8226 and MM1.R cells treated with indicated concentrations of **1** for 24 or 48 hours. Quantification was performed using the WST-1 assay (relative values ± SD and EC_{50s}; $n = 3$). (B) Gel-based competitive *in situ* profiling of targets of **1**. RPMI 8226 cells were treated with various concentrations of **1** for 6 h, lysed, and treated with 10 μM **14**. (C) Log_2 LFQ ratios of proteins identified from the *in situ* competitive pull-down experiment with 100 nM **1** or DMSO and with 10 μM **14** ($n = 6$, three biologicals and two technicals each). (D) Cellular targets of **1** (>50% competition) in RPMI 8226 cells. Quantification was performed using the label-free quantification (LFQ) method ($n = 6$).

We chose to further validate the engagement of PSMB2 (Proteasome 20S Subunit β2) and PSMB5 (Proteasome 20S Subunit β5) by **1**, because their chemical co-inhibition has been

shown to be particularly cytotoxic in proteasome inhibitor-resistant MM cells and has therefore emerged as a promising therapeutic strategy.[22] To confirm PSMB2 and PSMB5 as targets, both proteins were cloned as FLAG-tagged versions and overexpressed in HEK293T cells. PSMB2 and PSMB5-expressing cells were lysed and the lysates labeled with 30 µM **14** for 1 h, followed by conjugation to TAMRA azide, separation by SDS-PAGE, and visualization of probe-bound proteins by in-gel fluorescence scanning (**Figs. 4A**, **S2**). A new labeled band was clearly seen in the overexpressed lane of both gels, indicating successful labeling of both overexpressed proteins, PSMB2-F and PSMB5-F. Having confirmed both proteins as targets of cepafungin I, we successfully assigned the fluorescence bands in the gel profile of **14** to respective proteasome subunits as previously described[18,23,24] and quantified the *in situ* IC_{50} values of **1** for the endogenously expressed proteasome subunits, yielding IC_{50s} of 7.5 nM for PSMB5 and 35 nM for PSMB2 (**Figs. S3A, B**). Interestingly, these values only slightly deviate from previously reported IC_{50s} for inhibition of purified yeast proteasome subunits by **1** (PSMB5: 4 nM; PSMB2: 24 nM[4]). In order to gain more insight into the structure-activity relationship between **1** and PSMB5, we synthesized several derivatives of **1** (**Fig. 4**) and compared their ability to inhibit β5 activity in RPMI 8226 cells. Cells were treated with various concentrations of compounds for 6 hours, then lysed and treated with the fluorogenic β5 subunit-selective fluorogenic substrate Suc-LLVY-AMC.[25] Release of the 7-Amino-4-methylcoumarin (AMC) fluorophore via proteolytic cleavage by β5 was followed over time and quantified to obtain IC_{50} values (**Fig. 4B**). From all compounds tested, **1** most potently inhibited the β5 subunit activity. In agreement with prior work,[4] terminal methyl branching in **1** leads to a nearly fivefold increase in β5 inhibitory activity compared to **2** (glidobactin A). The difference in potency between **15** (desoxycepafungin) and **1**, over tenfold loss, is in agreement with a recently reported potency difference between **2** and its corresponding desoxy-macrocycle variant luminmycin A.[19] Additionally, **16** (saturated cepafungin) demonstrated a fourteen-fold loss in potency compared to **1**. These results suggest that the secondary alcohol on the macrocycle and the 2,4-dienamide motif on the tail region of **1** are critical for the β5 inhibitory activity.

Next, we sought to investigate if **1** mediates the expected biological downstream response similar to other proteasome inhibitors. One of the key cellular responses of proteasome inhibition is the accumulation of polyubiquitinated proteins, gradually leading to dysfunction and apoptosis.[26] Indeed, Western blot of lysates from **1**-treated RPMI 8226 cells using a mono-/poly-ubiquitin-conjugate specific antibody showed a concentration-dependent increase in ubiquitinated proteins (**Fig. 4C**). Next, we probed the same lysates by Western blot for Poly(ADP-Ribose) Polymerase (PARP-1) and observed PARP-1 cleavage in **1**-treated samples, indicating that **1** induced apoptotic cell death (**Fig. 4C**).[27] Finally, we performed a global proteomics experiment to identify proteins that accumulate or are upregulated in RPMI 8226 cells upon **1** treatment in comparison to the treatment with the clinical proteasome inhibitor drug bortezomib (BTZ). Cells were treated for 14 h with either **1** or BTZ at concentrations matching their corresponding EC_{50} values at the 24 h timepoint (**Figs. 3A, S4**). Cells were lysed, proteins digested, and peptides analyzed by LC-MS/MS. Out of 3700 quantified proteins, 88 proteins were significantly upregulated (FDR 0.05; S_0 0.01) in **1**-treated samples and 25 in BTZ-treated samples compared to DMSO control samples (**Figs. 4D**, **S5**; **Table S4**). Indeed, 19 of 25 proteins upregulated in BTZ-treated samples, were also upregulated in proteomic samples from **1**-treated cells, thus confirming highly similar mode of action for these two compounds. Notably, 11 out of these 19 common targets have previously been reported to be upregulated upon proteasome inhibition in general (HERPUD1,[28] KIAA0101, RRM2,[29] CDC6,[30] CCNB1,[31] NUSAP1,[32] ORC1,[33] CYBA,[34] CKAP2,[35] KRT18,[36] TPX2[37]) and 5 more targets (BAG3,[38] SRXN1, HMOX1, SQSMT1,[39] HSPA1A/B[40]) specifically upon bortezomib treatment. Altogether, our data show that **1** is a potent and highly selective covalent inhibitor of the 20S proteasome that mediates downstream effects similar to the clinical drug BTZ in multiple myeloma cells.

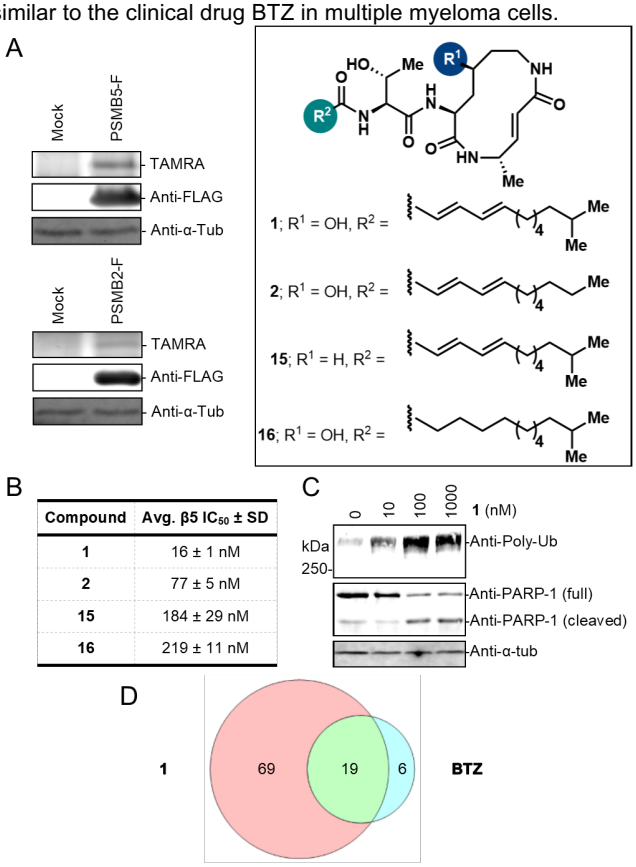

Figure 4. Validation of target engagement, structure-activity relationship, and downstream effects of **1**. (A) Labeling of mock and overexpressed PSMB2-FLAG and PSMB5-FLAG in HEK293T lysate with 30 µM **14**. Shown are the TAMRA fluorescence profile of **14** (top), Western blot membrane probed for FLAG (middle), and α-tubulin as a loading control (bottom). See also Fig. **S2**. (B) *In situ* inhibition of chymotrypsin-like (β5) proteasome activity by **1** and its derivatives. RPMI 8226 cells were treated with various concentrations of compounds for 6 h, lysed, treated with 100 µM fluorogenic substrate Suc-LLVY-AMC, and incubated for 2 hours at 37 °C. IC_{50} values were quantified based on $A_{360}ex/A_{460}em$ readouts (n = 3). (C) Western blotting of lysates obtained from RPMI 8226 cells treated with various concentrations of **1** for 6 h. Membranes were probed for mono- and poly-ubiquitin, PARP-1, and α-tubulin as a loading control. (D) Venn diagram representing the overlap in significantly upregulated proteins (FDR 0.05; S_0 0.01) upon 14 h treatment of RPMI 8226 cells with 100 nM **1** or 2.5 nM BTZ versus vehicle. Quantification was performed using label-free quantification (LFQ) method (n = 6).

Conclusion

By harnessing the ability of GlbB to hydroxylate L-lysine in a selective and efficient fashion, we have developed a concise chemoenzymatic synthesis of cepafungin I. Despite challenges in the late-stage macrocyclization and amide coupling steps, cepafungin I could be obtained in *ca.* 8% yield over 9 steps (longest linear sequence). The modularity of this route allowed the development of a chemoproteomic probe to interrogate the cellular targets of cepafungin I. Our chemoproteomics studies revealed that cepafungin I is able to covalently engage 20S proteasome subunits PSMB2 and PSMB5 with exceptional selectivity and that cepafungin I elicit many similar downstream biological responses to the clinically-approved proteasome inhibitor drug bortezomib. Contemporaneous to our efforts, Böttcher and co-workers reported the development of an activity-based probe by derivatization of syringolin A that was obtained from its native producer and showed the ability of the syrbactins to coinhibit PSMB2 and PSMB5 with high potency.[19] Complementary to Böttcher's findings, our work provides the first proteome-wide identification of syrbactin protein targets in cancer cells and validation of their downstream biological effects via in-depth quantitative proteomics analyses. Moreover, the synthetic strategy developed herein enabled access to both natural and unnatural cepafungin analogs for initial structure-activity relationship studies. Especially notable in this regard is the observation that the macrocyclic secondary alcohol, as well as the degree of unsaturation and the terminal branching of the lipid tail, are critical for high inhibitory potency. Further medicinal chemistry exploration featuring the use of other hydroxylated amino acids[41] and alternative lipid tails is ongoing in our laboratory.

Acknowledgements

This work is supported, in part, by the National Institutes of Health Grant GM128895 (H.R.). We acknowledge the Bannister lab and the Shen lab for generous access to their instrumentation. We acknowledge Dr. D. Abegg for valuable discussions and proofreading of the manuscript. We thank P. Dickson and the Kodadek lab for providing the cell lines used in this study and for their valuable suggestions.

Keywords: syrbactin • natural product • proteasome inhibitor • covalent inhibitor • chemoproteomics

[1] D. Krahn, C. Ottmann, M. Kaiser, *Nat. Prod. Rep.* **2011**, *28*, 1854–1867.

[2] (a) M, Oka, Y. Nishiyama, S. Ohta, H. Kamei, M. Konish, T. Miyaki, T. Oki, H. Kawaguchi, *J. Antibiot.* **1988**, *41*, 1331–1337; (b) J. Shoji, H. Hinoo, T. Kato, T. Hattori, K. Hirooka, K. Tawara, O. Shiratori, Y. Terui, *J. Antibiot.* **1990**, *43*, 783–787.

[3] M. Groll, B. Schellenberg, A. S. Bachmann, C. R. Archer, R. Huber, T. K. Powell, S. Lindow, M. Kaiser, R. A. Dudler, *Nature* **2008**, *452*, 755–758.

[4] M. L. Stein, P. Beck, M. Kaiser, R. Dudler, C. F. W. Becker, M. Groll, *Proc. Natl. Acad. Sci. USA* **2012**, *109*, 18367–18371.

[5] T. A. Guerrero-Garcia, S. Gandolfi, J. P. Laubach, T. Hideshima, D. Chauhan, C. Mitsiades, K. C. Anderson, P. G. Richardson, *Expert Rev. Proteomics* **2018**, *15*, 1033–1052.

[6] C. R. Archer, M. Groll, M. L. Stein, B. Schellenberg, J. Clerc, M. Kaiser, T. P. Kondratyuk, J. M. Pezzuto, R. Dudler, A. S. Bachmann, *Biochemistry* **2012**, *51*, 6880–6888.

[7] E. S. Weyburne, O. M. Wilkins, Z. Sha, D. A. Williams, A. A. Pletnev, G. de Bruin, H. S. Overkleeft, A. L. Goldberg, M. D. Cole, A. F. Kisselev, *Cell. Chem. Biol.* **2017**, *24*, 218–230.

[8] R. Oerlemans, N. E. Franke, Y. G. Assaraf, J. Cloos, I. Van Zantwijk, C. R. Berkers, G. L. Scheffer, K. Debipersad, K. Votjekova, C. Lemos, J. W. van der Heijden, B. Ylstra, G. J. Peters, G. L. Kaspers, B. A. Dijkmans, R. J. Scheper, G. Jansen, *Blood* **2008**, *112*, 2489–2499.

[9] U. Schmidt, A. Kleefeldt, R. Mangold, J. Chem. Soc. Chem. Commun. 1992, 1687–1689.

[10] (a) T. Chiba, H. Hosono, K. Nakagawa, M. Asaka, H. Takeda, A. Matsuda, S. Ichikawa, *Angew. Chem. Int. Ed.* **2014**, *53*, 4836–4839; (b) S. Kitahata, F. Yakushiji, S. Ichikawa, *Chem. Sci.* **2017**, *8*, 6959–6963; (c) S. Kitahata, T. Chiba, T. Yoshida, M. Ri, S. Iida, A. Matsuda, S. Ichikawa, *Org. Lett.* **2016**, *18*, 2312–2315.

[11] M. C. Pirrung, G. Biswas, T. R. Ibarra-Rivera, *Org. Lett.* **2010**, *12*, 2402–2405.

[12] C. Dai, C. R. J. Stephenson, *Org. Lett.* **2010**, *12*, 3453–3455.

[13] (a) M. Oka, K. Yaginuma, K. Numata, M. Konishi, T. Oki, H. Kawaguchi, *J. Antibiot.* **1988**, *41*, 1338–1350; (b) M. Oka, K.-I. Iwata, Y. Nishiyama, H. Kamei, M. Konishi, T. Oki, H. Kawaguchi, *J. Antibiot.* **1988**, *41*, 1812–1822; (c) J. Clerc, M. Groll, D. J. Illich, A. S. Bachmann, R. Huber, B. Schellenberg, R. Dudler, M. Kaiser, *Proc. Natl. Acad. Sci. USA* **2009**, *106*, 6507–6512; (d) J. Clerc, B. Schellenberg, M. Groll, A. S. Bachmann, R. Huber, R. Dudler, M. Kaiser, *Eur. J. Org. Chem.* **2010**, 3991–4003.

[14] A. Amatuni, H. Renata, *Org. Biomol. Chem.* **2019**, *17*, 1736–1739.

[15] Z. J. Kamiński, B. Kolesińska, G. Sabatino, M. Chelli, P. Rovero, M. Blaszczyk, M. L. Główka, A. M. Papini, *J. Am. Chem. Soc.* **2005**, *127*, 16912–16920.

[16] E. E. Manasanch, R. Z. Orlowski, *Nat. Rev. Clin. Oncol.* **2017**, *14*, 417–433.

[17] T. Hideshima, P. Richardson, D. Chauhan, V. J. Palombella, P. J. Elliott, J. Adams, K. C. Anderson, *Cancer Res.* **2001**, *61*, 3071–3076.

[18] D. J. Kuhn, Q. Chen, P. M. Voorhees, J. S. Strader, K. D. Shenk, C. M. Sun, S. D. Demo, M. K. Bennett, F. W. van Leeuwen, A. A. Chanan-Khan, R. Z. Orlowski, *Blood* **2007**, *110*, 3281–3290.

[19] A. Pawar, M. Basler, H. Goebel, G. O. Alvarez Salinas, M. Groettrup, T. Böttcher, *ACS Cent. Sci.* **2020** DOI:10.1021/acscentsci.9b01170.

[20] A. E. Speers, B. F. Cravatt, *Chem. Biol.* **2004**, *11*, 535–546.

[21] D. Abegg, R. Frei, K. Cerato, D. Prasad Hari, C. Wang, J. Waser, A. Adibekian, *Angew. Chem. Int. Ed.* **2015**, *54*, 10852–10857.

[22] A. Besse, L. besse, M. Kraus, M. Mendez-Lopez, J. Bader, B.-T. Xin, G. de Bruin, E. Maurits, H. S. Overkleeft, C. Driessen, *Cell Chem. Biol.* **2019**, *26*, 340–351.

[23] M. Altun, P. J. Galardy, R. Shringarpure, T. Hideshima, R. LeBlanc, K. C. Anderson, H. L. Ploegh, B. M. Kessler, *Cancer Res.* **2005**, *65*, 7896–7901.

[24] M. Britton, M. M. Lucas, S. L. Downey, M. Screen, A. A. Pletnev, M. Verdoes, R. A. Tokhunts, O. Amir, A. L. Goddard, P. M. Pelphrey, *Chem. Biol.* **2009**, *16*, 1278–1289.

[25] P. Maher, *Bio Protoc.* **2014**, *4*, e1028.

[26] J. Adams, *Nat. Rev. Cancer* **2004**, *4*, 349–360.

[27] S. H. Kaufmann, S. Desnoyers, Y. Ottaviano, N. E. Davidson, G. G. Poirier, *Cancer Res.* **1993**, *53*, 3976–3985.

[28] S. H. Hong, J. Kim, J.-M. Kim, S.-Y. Lee, D.-S. Shin, K.-H. Son, D. C. Han, Y. K. Sung, B.-M. Kwon, *Biochem. Pharmacol.* **2007**, *74*, 557–565.

[29] B. Fabre, I. Livneh, T. Ziv, A. Ciechanover, *Biochem. Biophys. Res. Commun*. **2019**, *517*, 188–192.

[30] F. Blanchard, M. E. Rusiniak, K. Sharma, X. Sun, I. Todorov, M. M. Castellano, C. Gutierrez, H. Baumann, W. C. Burhans, *Mol. Biol. Cell* **2002**, *13*, 1536–1549.

[31] M. Matondo, M. Marcellin, K. Chaoui, M.-P. Bousquet-Dubouch, A. Gonzalez-de-Peredo, B. Monsarrat, O. Burlet-Schiltz, *PROTEOMICS* **2017**, *17*, 1600089.

[32] P. Mertins, J. W. Qiao, J. Patel, N. D. Udeshi, K. R. Clauser, D. R. Mani, M. W. Burgess, M. A. Gillette, J. D. Jaffe, S. A. Carr, *Nat. Methods* **2013**, *10*, 634–637.

[33] Y. Tatsumi, S. Ohta, H. Kimura, T. Tsurimoto, C. Obuse, *J. Biol. Chem.* **2003**, *278*, 41528–41534.

[34] E. H. J. Yew, N. S. Cheung, M. S. Choy, R. Z. Qi, A. Y.-W. Lee, Z. F. Peng, A. J. Melendez, J. Manikandan, E. S.-C. Koay, L.-L. Chiu, W. L. Ng, M. Whiteman, J. Kandiah, B. Halliwell, *J. Neurochem.* **2005**, *94*, 943–956.

[35] K. U. Hong, Y. S. Park, Y.-S. Seong, D. Kang, C.-D. Bae, J. Park, *Mol. Cell. Biol.* **2007**, *27*, 3667–3681.
[36] R. Kwan, K. Looi, M. B. Omary, *Exp. Cell Res.* **2015**, *335*, 12–22.
[37] H. Chen, P. Mohan, J. Jiang, O. Nemirovsky, D. He, M. C. Fleisch, D. Niederacher, L. M. Pilarski, C. J. Lim, C. A. Maxwell, *Cell Cycle* **2014**, *13*, 2248–2261.
[38] P. Liu, B. Xu, J. Li, H. Lu, *FEBS Lett.* **2009**, *583*, 401–406.
[39] K. K. Starheim, T. Holien, K. Misund, I. Johansson, K. A. Baranowska, A.-M. Sponaas, H. Hella, G. Buene, A. Waage, A. Sundan, G. Bjørkøy, *Blood Cancer J.* **2016**, *6*, e446.
[40] S. P. Shah, A. K. Nooka, D. L. Jaye, N. J. Bahlis, S. Lonial, L. H. Boise, *Oncotarget* **2016**, *7*, 59727–59741.
[41] J. B. Hedges, K. S. Ryan, *Chem. Rev.* **2019**, DOI:10.1021/acs.chemrev.9b00408.